SUPPLEMENTARY MATERIAL

Supplementary Figures

Supplementary Tables

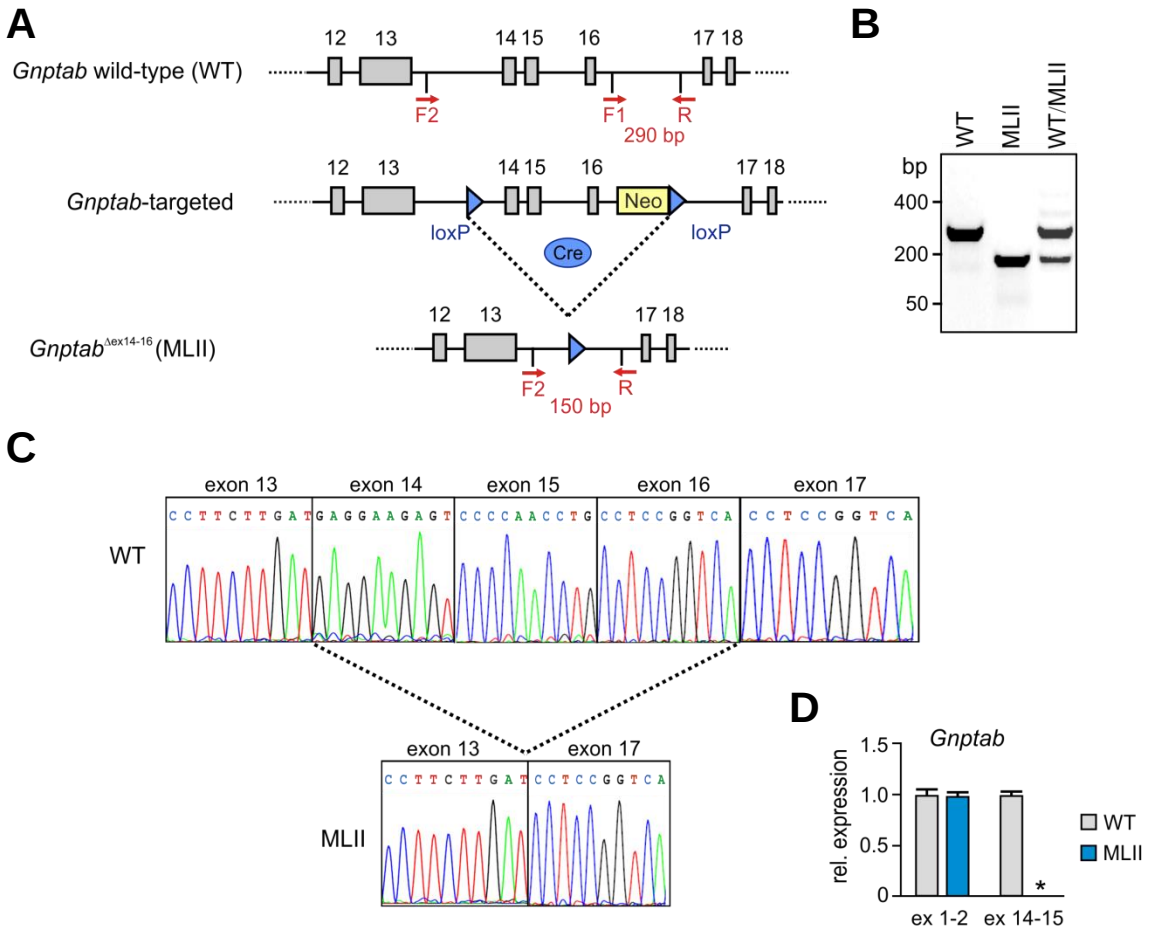

Fig. S1. Generation of MLII mice. (**A**) Schematic representation of the *Gnptab* wild-type (WT) allele from intron 12 to 18. The *Gnptab*-targeted allele contains a neomycin (Neo) resistance cassette between exons 16 and 17 to select for recombination in embryonic stem cells and two loxP sites in introns 13 and 16. Targeted embryonic stem cells were injected into blastocysts and implanted into the uterine horns of foster mothers. Chimeric offspring animals were crossed with Cre-expressing mice resulting in mice carrying the *Gnptab*$^{\Delta ex14\text{-}16}$ allele without exons 14, 15 and 16 and the Neo cassette (MLII^{Cre}). (**B**) PCR-mediated genotyping resulted in a 290 bp fragment for the *Gnptab* WT allele and a 150 bp fragment for the *Gnptab*$^{\Delta ex14\text{-}16}$ allele. Primer binding sites are indicated in (A) by red arrows. (**C**) RNAs were isolated from livers of 2-month-old mice of WT and MLII mice and used for cDNA synthesis. Sequencing confirmed the deletion of exons 14-16 in the cDNA of MLII mice. (**D**) Relative *Gnptab* mRNA levels were determined by quantitative PCR using TaqMan™ primers specific for exons 1-2 or exons 14-15 and normalized to *Actb* mRNA expression (WT = 1, mean ± SD, **p* ≤ 0.05).

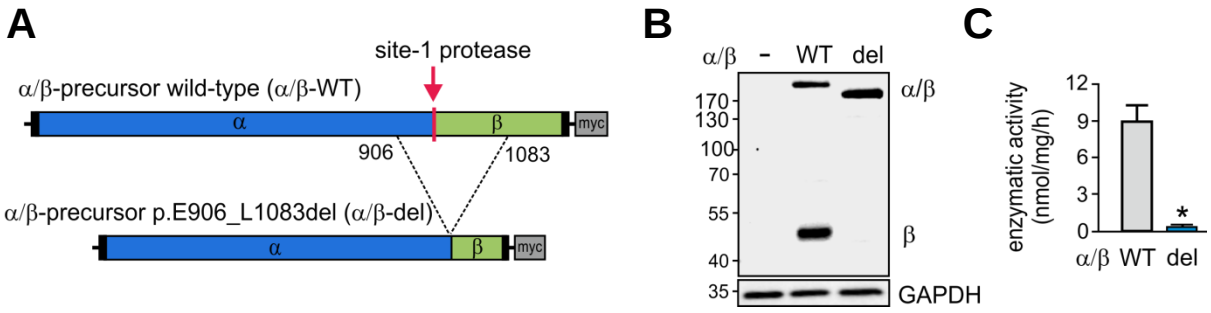

Fig. S2. Deletion of the S1P cleavage site prevents GlcNAc-1-phosphotransferase activity. (**A**) Schematic representation of human myc-tagged wild-type (WT) and p.E906_L1083del mutant α/β-precursors. The position of the deletion (amino acids 906 to 1083) is indicated by a dotted line. (**B**-**C**) HEK-293 cells were transiently transfected with cDNA encoding α/β-WT or mutant α/β-del. (**B**) Cell extracts were processed by SDS-PAGE and anti-myc immunoblot analysis detecting α/β-precursors (α/β) and β-subunits (**B**). GAPDH and extracts of non-transfected cells were used as loading and negative control, respectively. (**C**) GlcNAc-1-phosphotransferase activities (nmol/mg/h) towards α-methylmannoside were measured in extracts corresponding to 100 µg total protein, in a reaction lasting for 60 min (mean ± SD, **p* ≤ 0.05, n = 3).

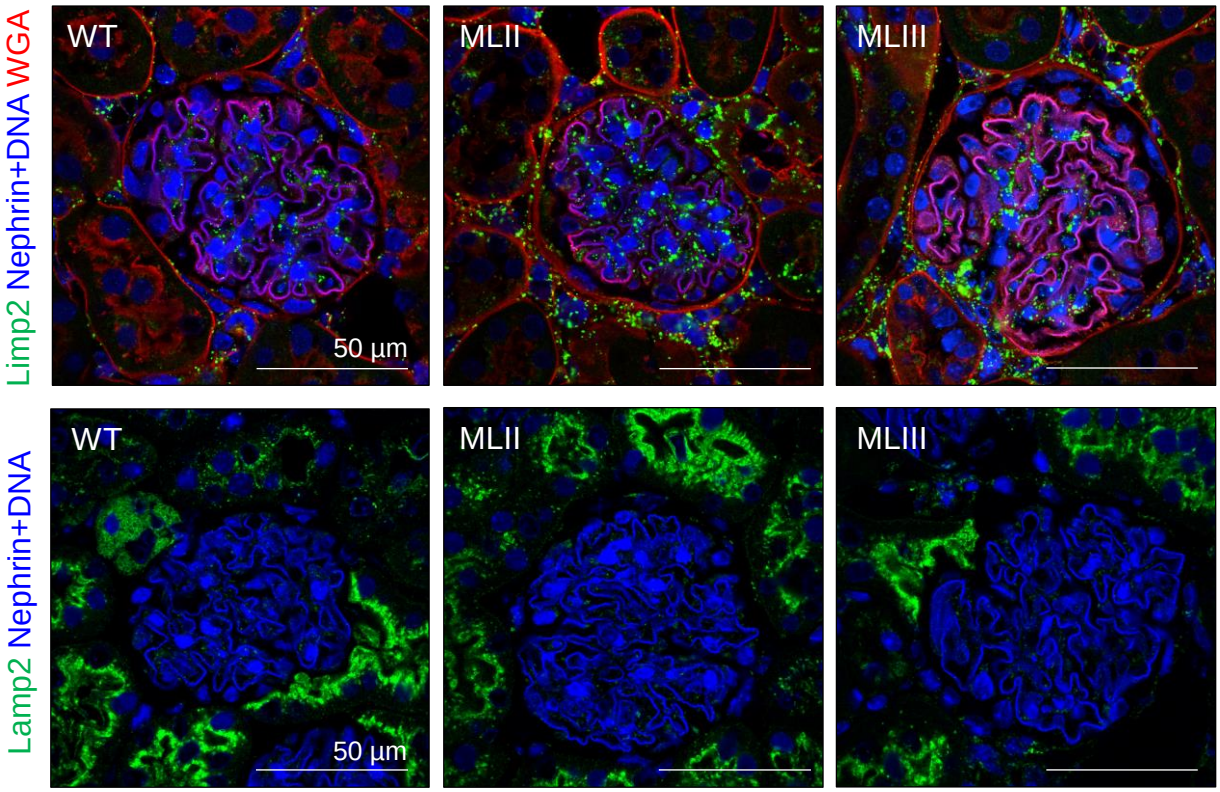

Fig. S3. Differential involvement of Lamp2-positive and Limp2-positive lysosomes in MLII and MLIII kidneys. Confocal micrographs exhibiting Limp2+ and Lamp2+ lysosomes (both green) at 40 weeks-of-age in MLII and 90 weeks-of-age in MLIII mice in comparison to a wildtype littermate. Glomerular filtration barrier was visualized by staining for the slit membrane protein nephrin (blue, linear staining in glomeruli), DNA (blue), Wheat germ agglutinin (WGA, red) was used to demarcate Limp2+ tubulointerstitial cells. Arrows point toward the endothelial cell lining of the glomerular filtration barrier, p = podocyte nucleus. Note the enlarged Limp2+ lysosomes in MLII and MLIII mice and the normal appearance of Lamp2+ lysosomes.

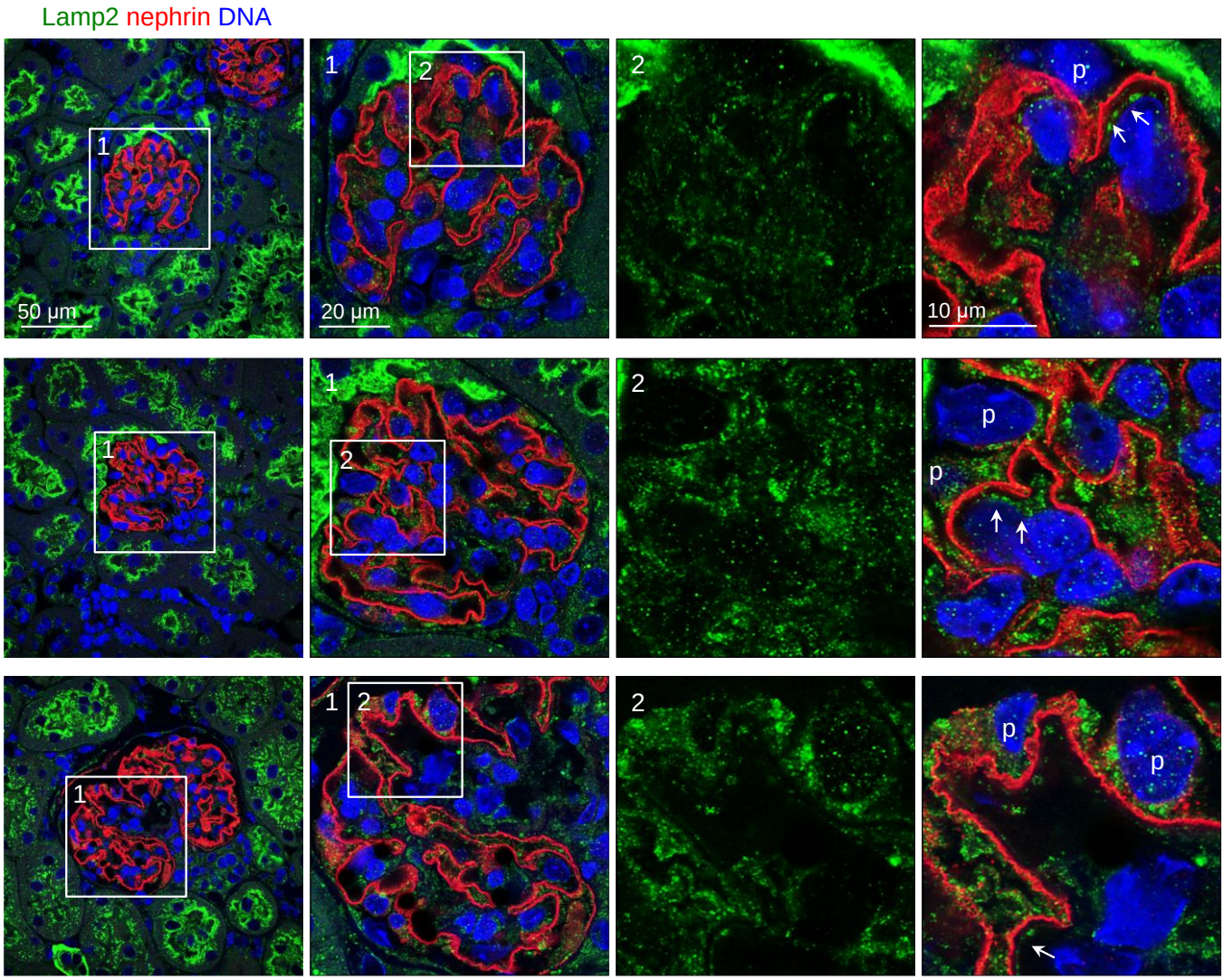

Fig. S4. MLII and MLIII mice exhibit more Lamp2+ lysosomes in glomerular cells. High-resolution confocal micrographs exhibiting Lamp2-positive lysosomes (green) at 40 weeks-of-age in MLII and 90 weeks-of-age in MLIII mice in comparison to a wildtype littermate. Glomerular filtration barrier was visualized by staining for the slit membrane protein nephrin (red), DNA (blue). Arrows point toward the endothelial cell lining of the glomerular filtration barrier, p = podocyte nucleus.

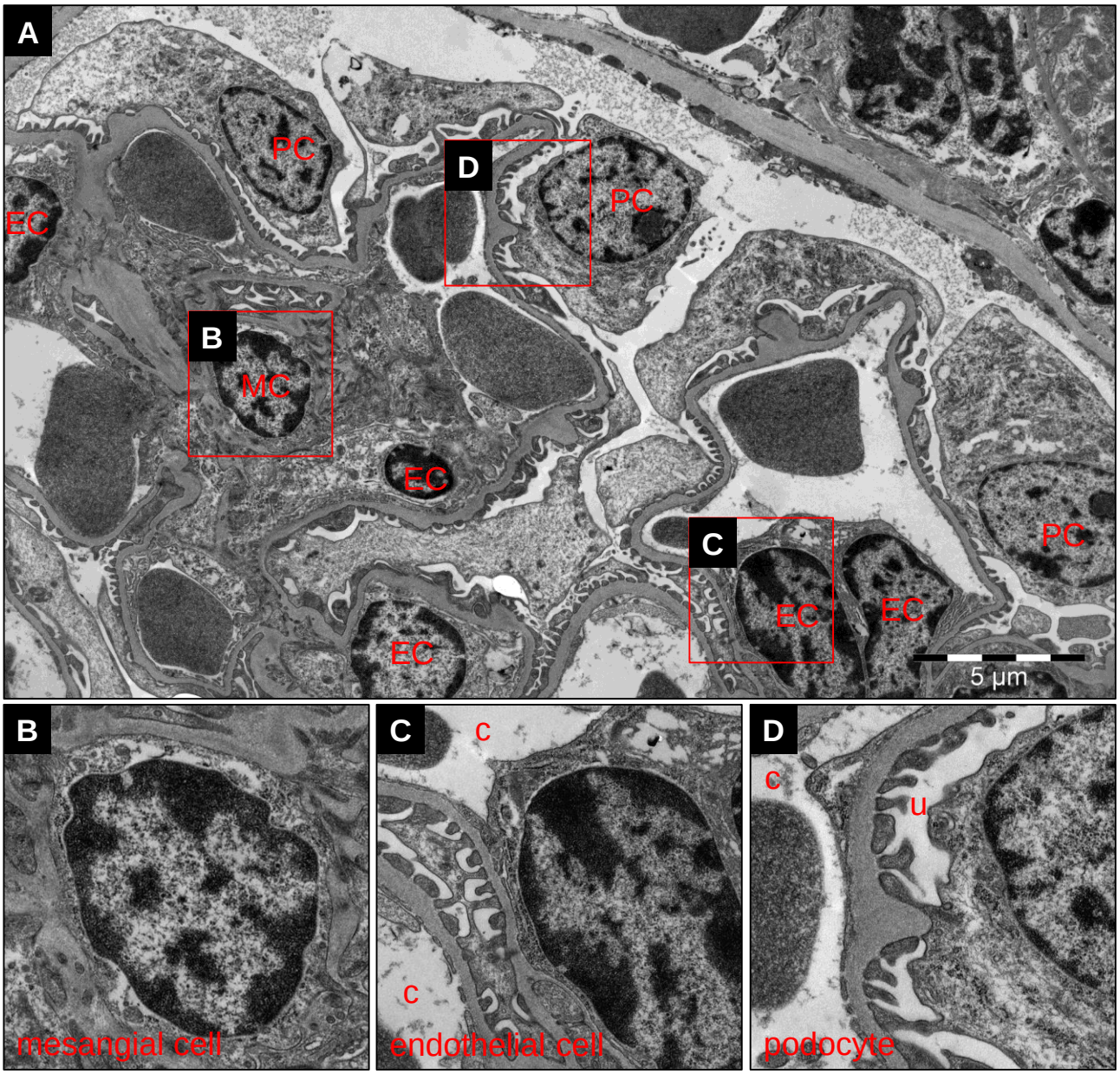

Fig. S5. Glomerular cells of wildtype littermates exhibit normal morphology. Electron microscopic evaluation of wildtype littermate glomeruli exhibit a normal cellular ultrastructure. Capillary space (c), urinary space (u), podocyte (PC), mesangial cell (MC), endothelial cell (EC).

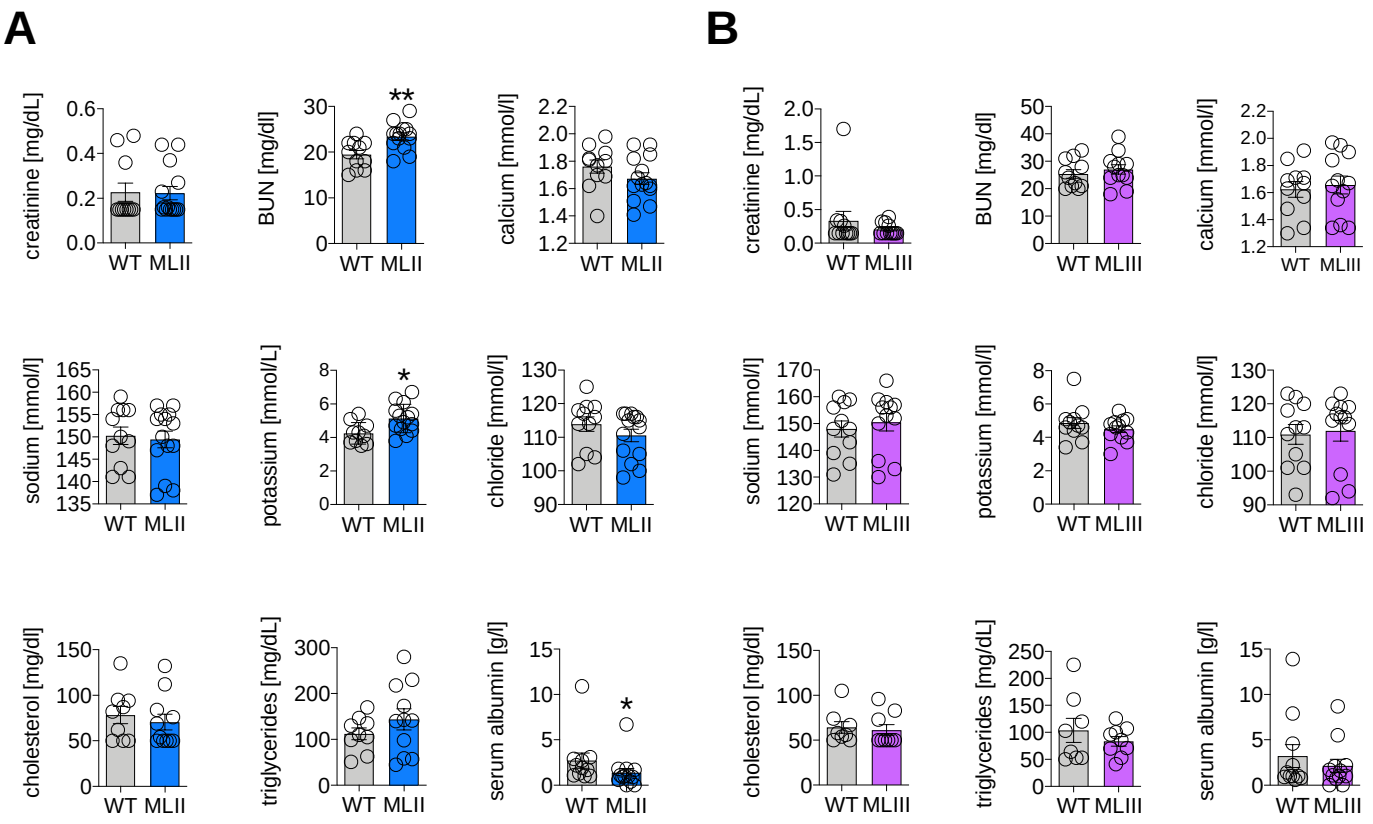

Fig. S6. Mucolipidosis type II and type III mice exhibit mostly normal serum parameters. Serum parameters for renal function were determined by automated measurement in 30-40 week old MLII (**A**), 60-90 week old MLIII (**B**) and wildtype (WT) littermates (mean ± SEM, Mann Whitney U test, n ≥ 11, four pooled independent experiments, **p* ≤ 0.05, ***p* ≤ 0.01).

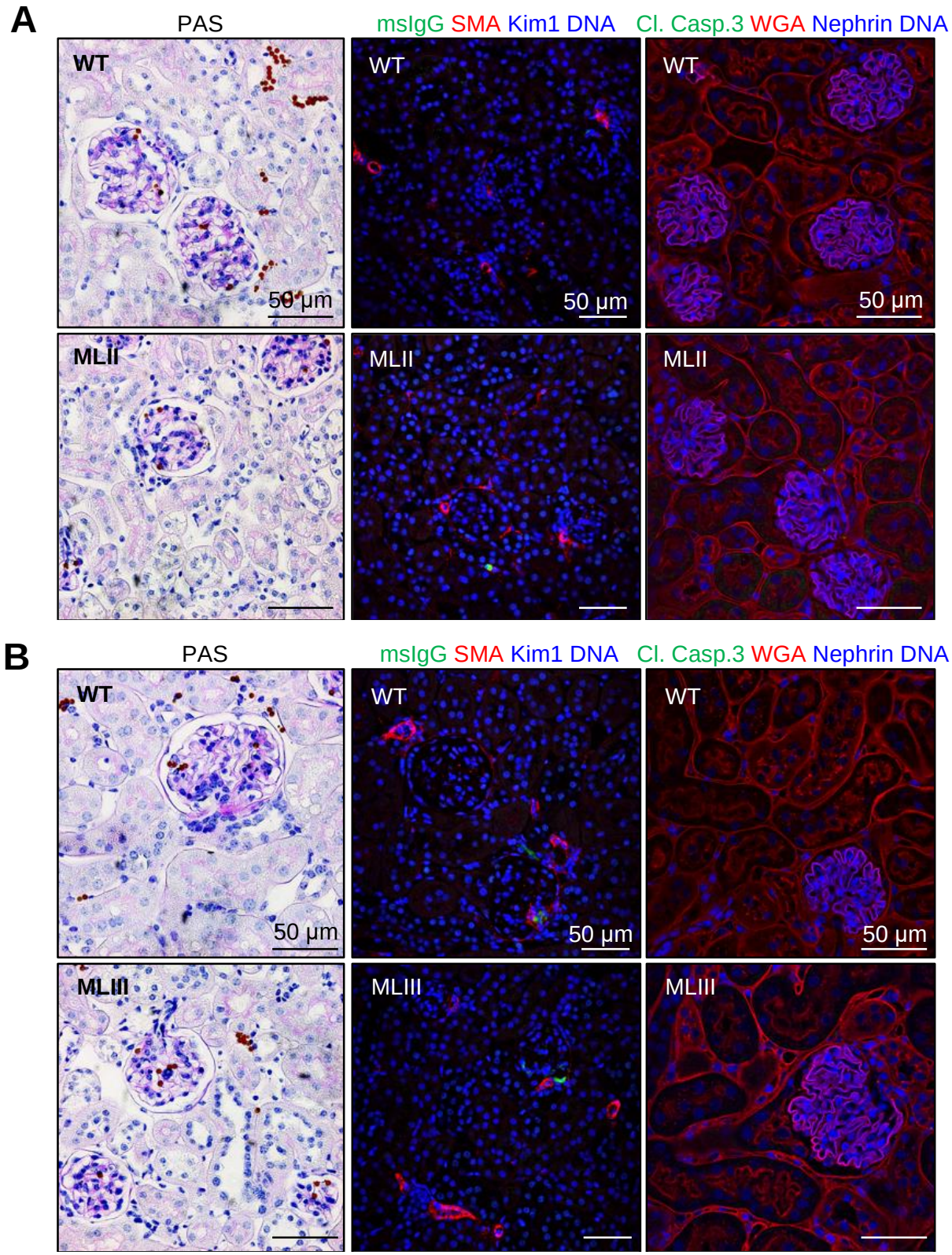

Fig. S7. Mucolipidosis type II and type III mice exhibit normal renal morphology. 30-40 week old MLII (**A**), 60-90 week old MLIII (**B**) and wildtype (WT) littermates showed normal cortical morphology by periodic acid staining (PAS), absence of mouse IgG (msIgG) deposition, absence of renal fibrosis (smooth muscle actin, SMA), absence of tubular injury (kidney injury molecule 1, Kim1), and absence of apoptosis (cleaved caspase 3) by light and confocal microscopy.

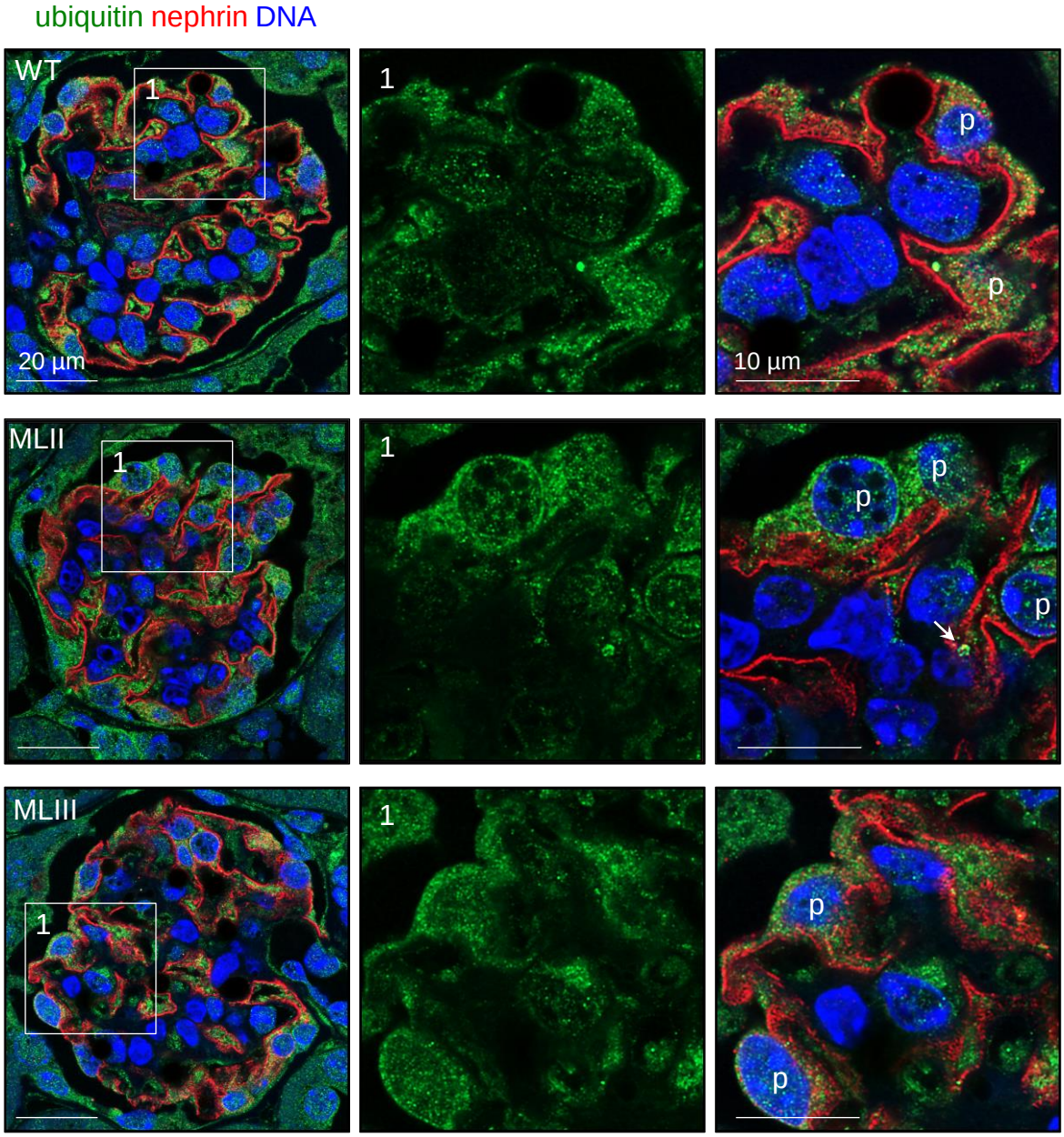

Fig. S8. Podocytes of MLII mice occasionally exhibit ubiquitin aggregates. Confocal micrographs of immunofluorescent stainings for ubiquitin (green) exhibit enhanced signal in podocytes (p) only of all glomerular cells in a 40-week-old MLII, 90-week old MLIII, and a littermate control mouse. No altered glomerular ubiquitin staining can be appreciated besides the occasional occurrence of ubiquitin aggregates (white arrow) in MLII podocytes.

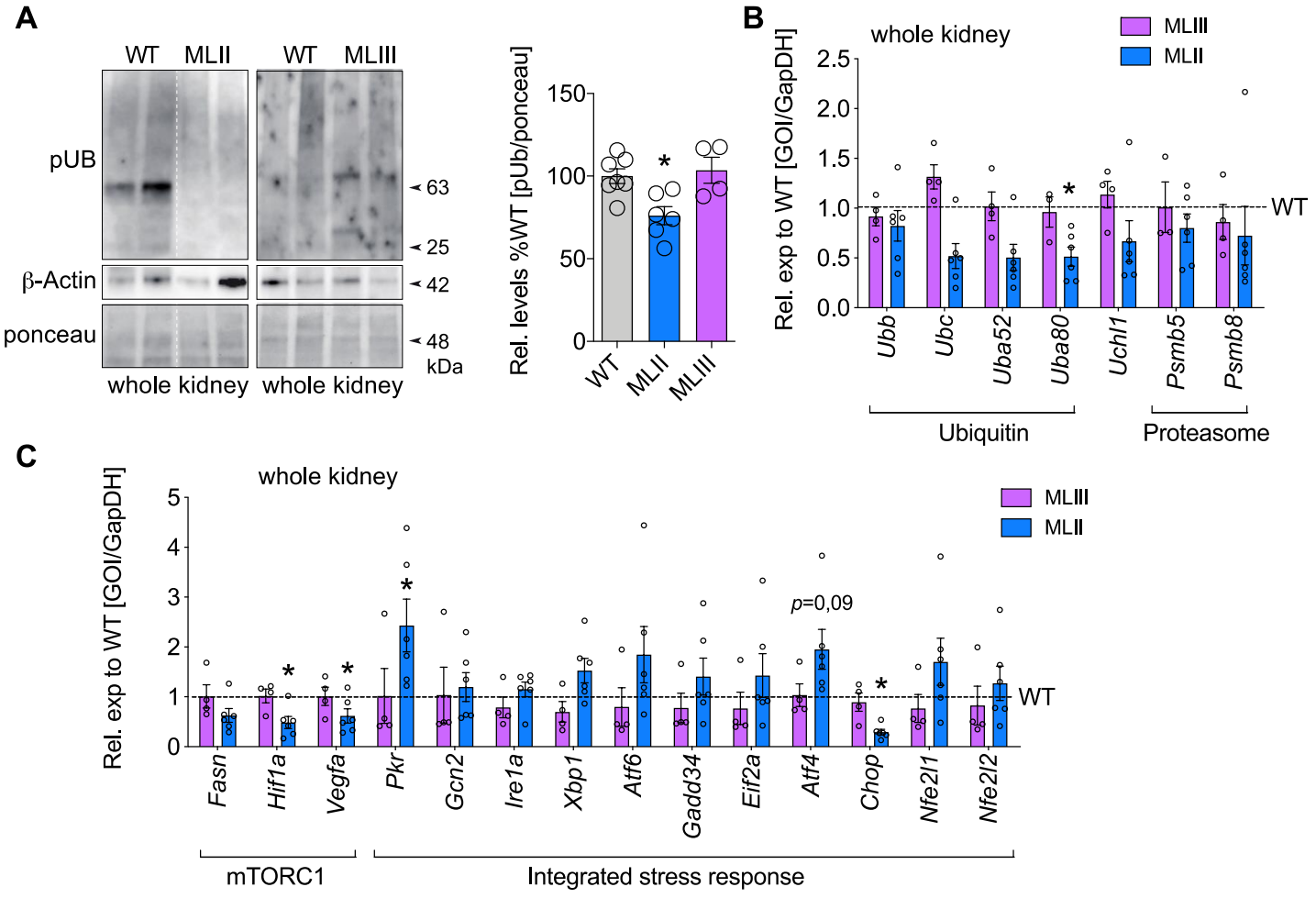

Fig. S9. Whole kidneys of MLII mice exhibit decreased ubiquitin protein and mRNA levels and transcriptional downregulation of protein translation pathways. (**A**) Ubiquitin levels of total kidney lysates of MLII mice (30-40 weeks of age) and MLIII mice (60-90 weeks of age) were analyzed by Western blot. Graph exhibits densitometric analysis of % pUB levels normalized to ponceau of the same membrane to wildtype (WT) littermates; mean ± SEM, Mann Whitney U test, n ≥ 3-6. (**B**) Total kidney transcript levels assessing the relative levels of the ubiquitin transcripts *Ubb*, *Ubc*, *Uba52*, and *Uba80*; of the deubiquitinating enzyme *Uchl1*; and of the proteasome subunits *Psmb5* (encoding for β5 of the standard proteasome) and *Psmb8* (encoding for LMP7 of the immunoproteasome) by qPCR in 60-90 week old MLIII and 30-40 week old MLII mice (relative expression of gene of interest (GOI) to respective wildtype (WT) littermate controls (black dashed line); mean ± SEM, Mann Whitney U test, n ≥ 3-6). Note the decrease of most ubiquitin transcripts in MLII mice and not in MLIII mice. (**C**) Total kidney transcript levels assessing the relative levels of the mammalian target of rapamycin complex 1 (mTORC1) dependent transcripts and of transcripts indicating activation of the integrated stress response by qPCR in 60-90 week old MLIII and 30-40 week old MLII mice (relative expression of gene of interest (GOI) to respective wildtype (WT) littermate controls (black dashed line); mean ± SEM, Mann Whitney U test, n ≥ 3-6). Note the decrease of most mTORC1-dependent transcripts and the activation of the integrated stress response in MLII kidneys but not in MLIII kidneys.

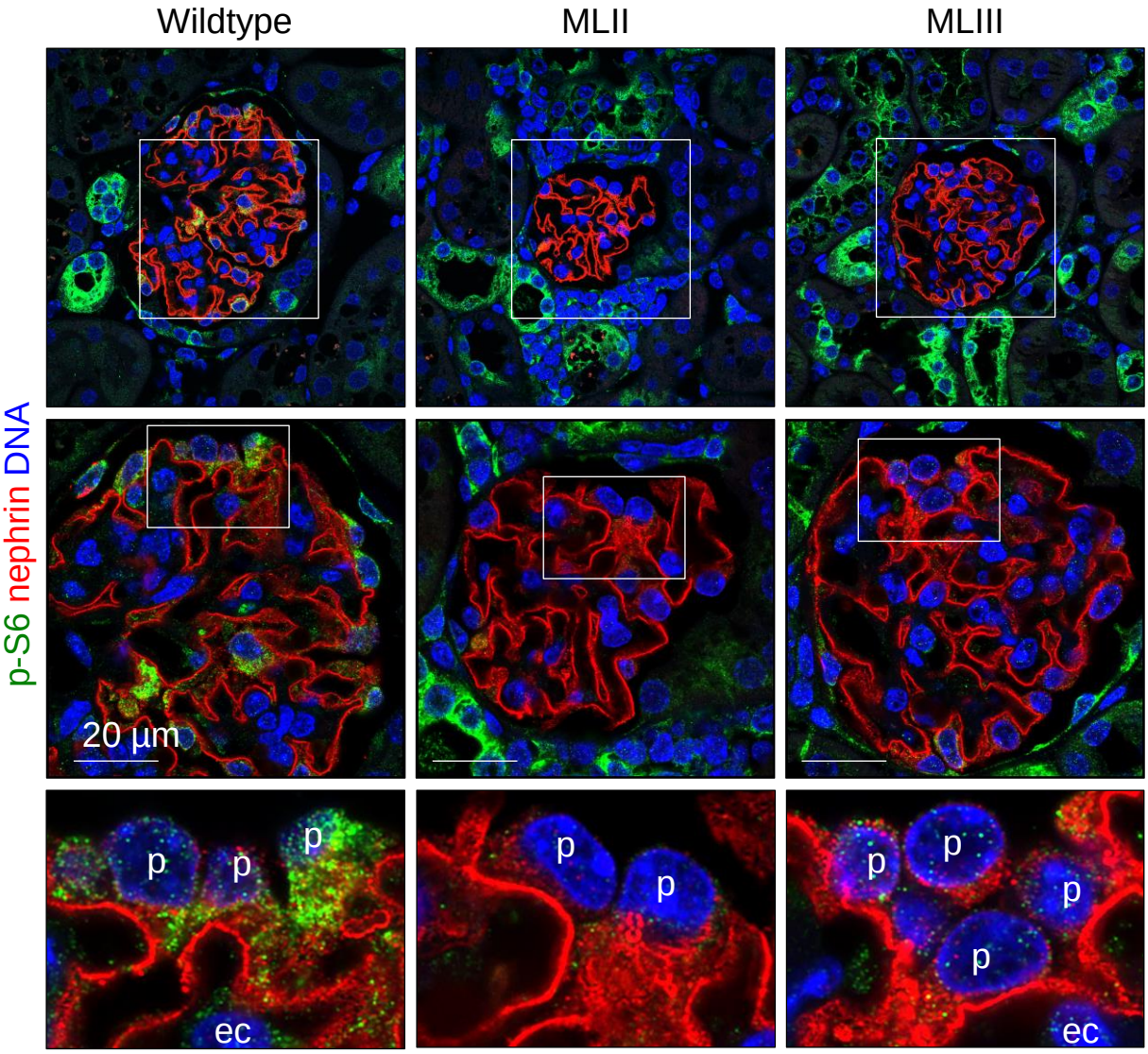

Fig. S10. Decreased mTORC1 activity in glomerular cells of mucolipidosis type II and type III mice. MLII mice (30-40 weeks of age) and MLIII mice (60-90 weeks of age) were analyzed for the expression levels of the mTORC1 target S6 in its phosphorylated form (p-S6) by high-resolution confocal microscopy. Note that podocyte (p) p-S6 levels are strongly reduced in both MLII and MLIII mice; endothelial cell (ec). In the tubulointerstitium, p-S6 expression is enhanced in MLII and MLIII mice.

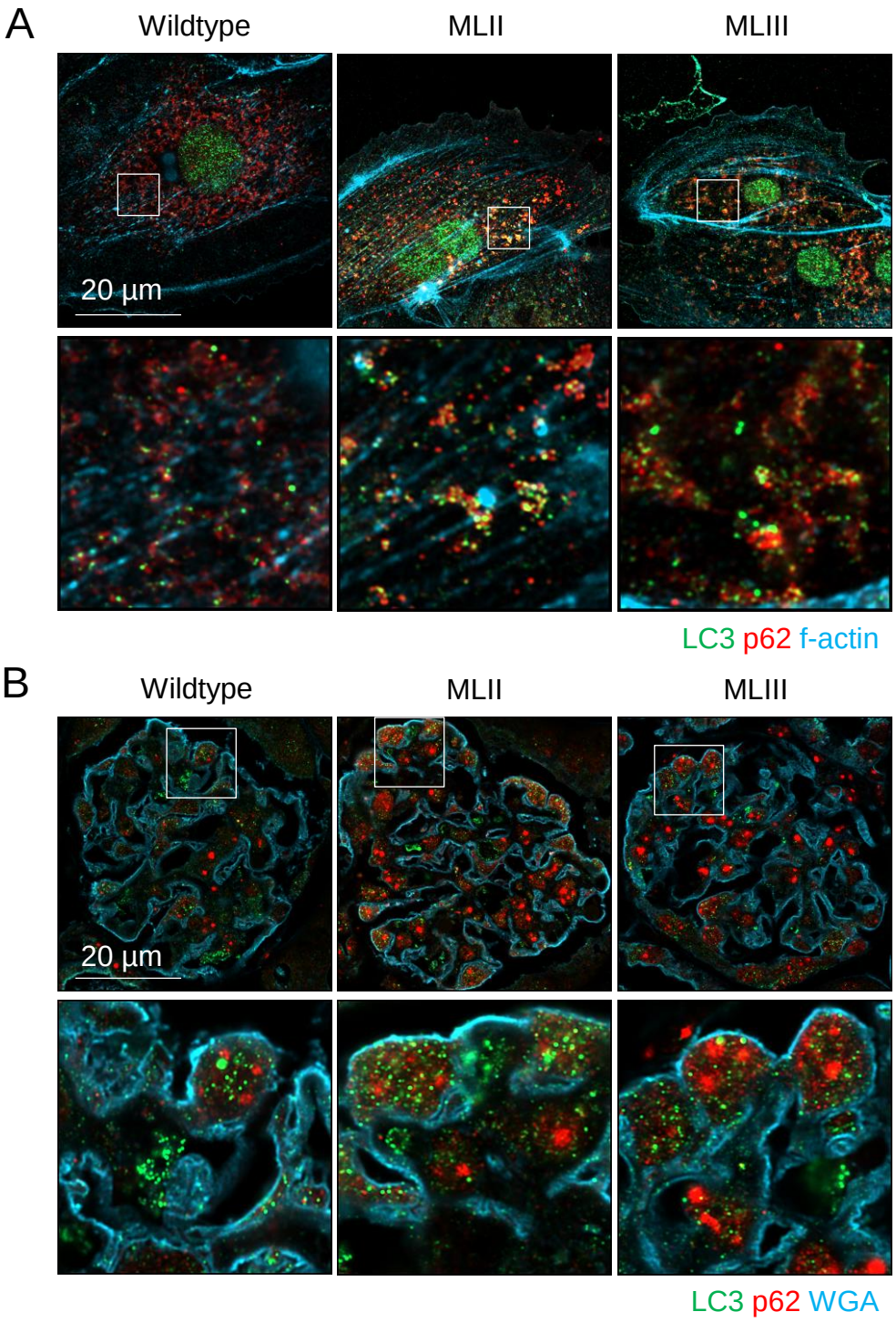

Fig. S11. Autophagy is impaired in MLIII and MLII glomerular cells. (A) Primary culture podocytes derived from MLIII, MLII and control littermates were stained for the ubiquitin receptor p62 (red), which shuttles ubiquitinated proteins to autophagosomes (demarcated by LC3, green) for degradation. Filamentous (f)-actin is stained in light blue. (B) High resolution confocal micrographs for p62 (red), LC3 (green), wheat germ agglutinin (light blue) to demarcate the glycocalix of MLIII and MLII glomerular cells in relation to a wild type control littermate. Note the increase in LC3 positive autophagosomes and the accumulation of p62 at LC3 positive lysosomes in primary culture podocytes, as well as in glomerular cells in relation to a control littermate of MLIII and MLII mice .

Forward primer		Reverse primer	
***Fasn*-fw**	5'GTT GGC CCA GAA CTC CTG TA3'	***Fasn*-rev**	5'GTC GTC TGC CTC CAG AGC3'
***Hif1a*-fw**	5'AAA CTT CAG ACT CTT TGC TTC G3'	***Hif1a*-rev**	5'CGG CGA GAA CGA GAA GAA3'
Vegfa-fw	5'AAT GCT TTC TCC GCT CTG AA3'	***Vegfa-rev***	5'GCT TCC TAC AGC ACA GCA GA3'
***Atf4*-fw**	5'CGG CAA GGA GGA TGC CTT3'	***Atf4*-rev**	5'TGG TTT CCA GGT CAT CCA TT3'
Atf6-fw	5'CCT GTG GCT TGT GGG TGT T3'	**Atf6-rev**	5'TCT ACT TGG TCC ATC GTG GG3'
***Chop*-fw**	5'GAA CCT GAG GAG AGA GTG TT3'	***Chop*-rev**	5'TAT AGG TGC CCC CAA TTT CA3'
***Pkr*-fw**	5'ACA AAT CGT GAC CGG AGT GG3'	***Pkr*-rev**	5'CAG GTC GGT CCT TGG GTT TC3'
***Gadd34*-fw**	5'AGA GAA GCC AGA ATC ACC TT3'	***Gadd34*-rev**	5'AGT GTA CCT TCC GAG CTT TT3'
Xbp1*-fw	5'AGT GTA CCT TCC GAG CTT TT3'	***Xbp1*-rev***	5'GGC AAC AGT GTC AGA GTC C3'
***Gcn2*-fw**	5'TGC CCA CCT ACA TAC CCA GA3'	***Gcn2*-rev**	5'TCA TCA CCT CTC CAC ACT GC3'
***Ire1a*-fw**	5'TGT GGT CAA GAT GGA CTG GC3'	***Ire1a*-rev**	5'GCT CGT GCC AGT AGT AGG TC3'
Eif2a-fw	5'GCA AAC AAT GTC CCA TCC TT3'	***Eif2a-rev***	5'GGA CCA CCA CAC TTC ACA GA3'
Nfe2l1-fw	5'CAA AGT GTC CCC TCA CCA GT3'	***Nfe2l1-rev***	5'AAT GAA CCC AAG ATG CCA AAG3'
Nfe2l2-fw	5'CTC GAG CTA CTC GGG TCA AC3'	***Nfe2l2-rev***	5'ACC CAG TGG ACA AGA CAA GG3'
***Psmb5*-fw**	5'TAA GCA TAC ACG GAG CCA GA3'	***Psmb5*-rev**	5'TGT GGC TGG GAT AAG AGA GG3'
***Psmb8*-fw**	5'ACC AAA GGA CCT CAG GAA TG3'	***Psmb8*-rev**	5'GGA CCC GGG ACA CTA CAG TT3'
***Ubb*-fw**	5'GCC GGC AAG CAG CTG GAA GA3'	***Ubb*-rev**	5'ACG GAG GAC CAG GTG CAG GG3'
***Ubc*-fw**	5'GAC GTC CAA GGT GAT GGT CT3'	***Ubc*-rev**	5'TCC AGA AAG AGT CCA CCC TG3'
***Uba52*-fw**	5'TCC AAG ACA AGG AAG GCA TC3'	***Uba52*-rev**	5'GCA AGG TGG ACT CTT TCT GG3'
***Uba80*-fw**	5'GGT TGA ACC CTC GGA CAC TA3'	***Uba80*-rev**	5'GCC ATC TTC CAG CTG CTT AC3'
***Uchl1*-fw**	5'AGC TGG AAT TTG AGG ATG GA3'	***Uchl1*-rev**	5'GGC CTC GTT CTT CTC GAA A3'
***18S*-fw**	5'CAC GGC CGG TAC AGT GAA AC3'	***18S*-rev**	5'AGA GGA GCG AGC GAC CAA A3'
***Gapdh*-fw**	5'GCC AAG GTC ATC CAT GAC AAT T3'	***Gapdh*-rev**	5'GAG GGG CCA TCC ACA GTC TT3'

*204bp and 178bp fragment on 2-3% agarose gel

Table S1: qPRC primer sequences against murine transcripts used in the study.

	#	sex	age (years)	creatinine (g/L)	albumin (mg/L)	ACR (mg/g)	Na+ (mmol/L)	K+ (mmol/L)	Ca2+ (mmol/L)	Cl- (mmol/L)	anorg. phosphate (mmol/L)
healthy control	**P1**	f	9	2,34	2,82	1,21	295	70,3	3,38	>330	11
	P2	f	13	1,15	0,92	0,80	134	33,7	1,27	151	7
	P3	f	16	3,79	3,05	0,80	168	120,2	2,78	288	18
	P4	f	23	0,77	1,79	2,34	72	37	<1,25	97	3
	P5	m	25	3,85	3,17	0,82	142	17,5	3,84	154	16
	P6	f	41	2,28	1,49	0,65	64	98,1	2,17	117	14
	P7	f	43	3,29	7,43	2,26	105	62,6	4,5	180	28
	P8	f	44	0,52	2,04	3,96	55	21,5	1,9	55	4
	P9	m	50	2,69	1,71	0,63	180	65,5	3,22	189	28
MLIII gamma	**P10**	m	12	3,92	3,74	0,96	284	41,7	>3,75	312	16
	P11	m	46	3,48	8,84	2,54	179	94,6	<1,25	274	>29
	P12	m	49	3,92	10,74	2,74	188	116,4	1,73	307	33
MLIII alpha/beta	**P13**	m	6	0,33	2,83	8,68	155	46,6	<1,25	179	13
	P14	m	12	1,96	1,07	0,54	116	69,9	-	195	10
	P15	f	13	4,17	4,56	1,09	90	50,3	3,43	144	27
	P16	f	21	4,80	9,07	1,89	143	65,6	-	162	19
	P17	m	34	3,73	13,37	3,59	179	85,2	4,43	238	27
MLII	**P18**	m	0,33	0,27	5,89	21,88	12	28,6	<1,25	19	6
	P19	m	0,66	1,08	68,89	63,67	39	123,7	1,97	50	>29
	P20	f	4	0,28	2,06	7,37	-	-	2,04	-	9

Table S2: Urine analysis of healthy controls (P1-P9), MLIII gamma (P10-P12), MLIII alpha/beta (P13-P17), and MLII patients (P18-P20). ACR = albumin creatinine ratio, f = female, m = male.